

Article

## Hot Ductility Loss in a Fe-Ni-Based Superalloy

Chen-Wei Li <sup>1</sup>, An-Chou Yeh <sup>1,\*</sup>, Chi-San Chen <sup>2</sup> and Woei-Ren Wang <sup>2</sup>

<sup>1</sup> Department of Material Science and Engineering, National Tsing-Hua University (NTHU), Hsinchu 30013, Taiwan; E-Mail: s9931117@m99.nthu.edu.tw

<sup>2</sup> Nanopowder and Thin Film Technology Center, ITRI-South, Industrial Technology Research Institute, Chutung 31040, Taiwan; E-Mails: chenchisan@itri.org.tw (C.-S.C.); woeiren\_wang@itri.org.tw (W.-R.W.)

\* Author to whom correspondence should be addressed; E-Mail: yehac@mx.nthu.edu.tw; Tel.: +886-3-5715131 (ext. 33897); Fax: +886-3-5722366.

Academic Editor: Johan Moverare

Received: 31 October 2015 / Accepted: 15 December 2015 / Published: 21 December 2015

---

**Abstract:** High temperature tensile tests have been conducted on samples of a Fe-Ni based superalloy, Incoloy A-286, and significant ductility loss has been observed at 1220 °C. Titanium-rich, thin-film-like phase has been found on the inter-granular facets of fracture surfaces. It appears that sulfur content of Ti-rich phase was higher than that of the matrix. At 1220 °C, liquation of Ti-rich phases has resulted in thin-film-like morphology along the grain boundary and caused the ductility loss during tensile deformation.

**Keywords:** superalloy; incoloy A-286; hot ductility loss

---

### 1. Introduction

Incoloy A-286 (A-286) is an iron-nickel base, austenitic superalloy containing 25 wt. % of Ni, 15 wt. % of Cr and other minor elements like Ti, Al and Mo. A-286 has a long service history in the gas turbine engine industry due to its strength and oxidation resistance at intermediate temperatures around 650 °C [1–4]. However, A-286 has been found to be prone to intergranular fracture when it is deformed at high temperatures [4,5]. The issue of hot ductility loss has attracted much attention in the superalloy industry, and numerous studies have been reported [6–11]. Most of these studies have suggested impurities segregations and formation of precipitates along grain boundaries to be

responsible for loss of ductility. For example, segregations of phosphorus and sulfur to grain boundaries have been observed to result decrease ductility significantly [12]. And, formation of Laves phase at 980 °C may also affect the ductility of A-286 [13]. However, limited literatures are available to describe the mechanism of ductility loss at temperatures above 1200 °C.

The present article aims to elucidate the underlying mechanisms of high temperature ductility loss for A-286 by examining the fracture surfaces after high temperature tensile tests with scanning electron microscope and transmission electron microscope analysis.

## 2. Experimental Procedure

An ingot of A-286 processed by vacuum induction melting and was supplied by Gloria Materials Technology Cooperation (Tainan, Taiwan), in as-solutioned condition, and the ingot was then subjected to standard ageing heat treatment at 750 °C for 16 h to induce precipitation of strengthening  $\gamma'$  phase. Cylindrical tensile specimens with a diameter of 6 mm and a length of 8 cm were machined from the ingot. High temperature tensile tests were conducted on Gleeble 3500 (Dynamic Systems Inc., Austin, TX, USA), at 1180, 1200 and 1220 °C with a constant strain rate of  $10^{-3} \text{ s}^{-1}$ . After the tensile tests, fractured specimens were taken for microstructure analysis.

The chemical composition of the as-received A-286 bar was analyzed via glow discharge spectrometer (GDS, LECO GDS-750A, St. Joseph, MI, USA), and listed in Table 1. The cross sections of the fractured specimens were examined by scanning electron microscope (SEM, Hitachi SU8010 FE-SEM, Tokyo, Japan) and its Energy Dispersive X-ray Spectrometer (EDAX). Focus ion beam system (FIB, JEOL JIB-4601F, Tokyo, Japan) was utilized to prepare specimens from fracture surface for transmission electron microscope analysis. Diffraction patterns and compositional analysis were conducted by transmission electron microscope (TEM, Philips Tecnai F30 FEG-TEM, Amsterdam, The Netherlands) and its EDAX spectrometer.

**Table 1.** Chemical composition of A286 specimens via GDS analysis in wt. %.

Element	Fe	Ni	Cr	Ti	Mn	Mo	Si	V	Al	Cu	C	P	S
wt. %	Balance	25.0	14.3	1.78	1.47	1.27	0.51	0.34	0.10	0.20	0.04	0.02	<0.01

## 3. Results and Discussion

Stress-strain curves are shown in Figure 1, and certain degree of work hardening can be observed before fracture for 1180 °C and 1200 °C conditions. It is obvious that both tensile strength and strain decrease with increasing testing temperature. Although the fracture strain at 1200 °C has been decreased by 50% from 1180 °C, 13% of strain is still considered as ductile fracture behavior. An increase in temperature can soften the material as indicated by the decrease in tensile strength; however, the ductility of A-286 has also been decreased dramatically. Interestingly, a near-zero ductility at 1220 °C indicates a brittle fracture behavior at this temperature.

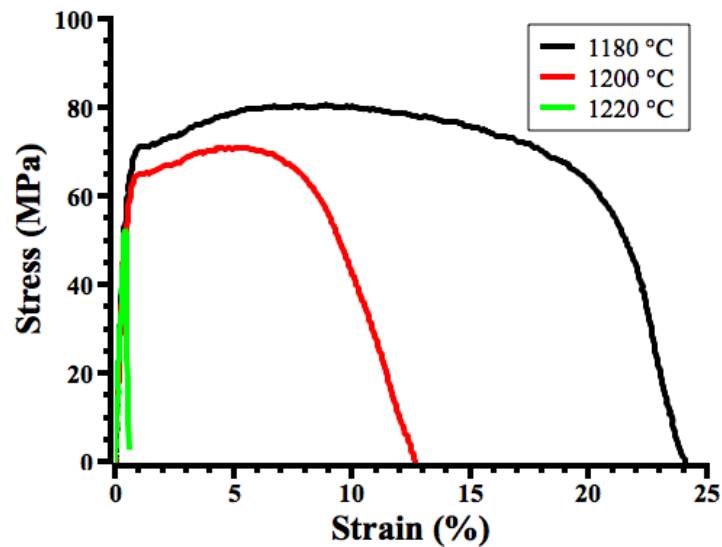


**Figure 1.** The stress-strain curve for A-286 specimens tested at different temperatures.

Fracture surfaces after tensile tests are shown in Figure 2. A typical ductile fracture surface with majority of dimple features can be observed for the 1180 °C condition, Figure 2a. A mixture of dimple and sharp cleavage surfaces can be seen for the 1200 °C condition, Figure 2b. For 1220 °C condition, inter-granular fracture surface can be seen mainly indicating that it is brittle fracture mode, Figure 2c, and there appears to be some cavities on the grain facets.

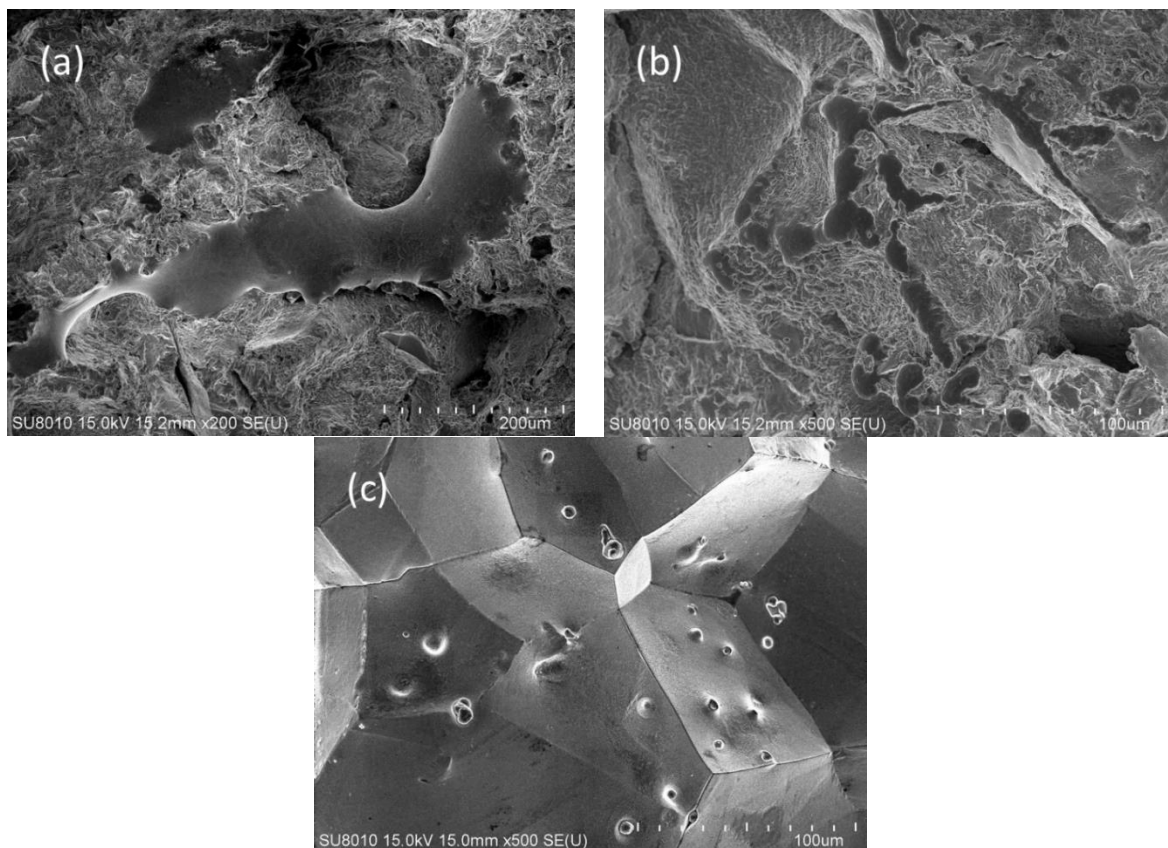


**Figure 2.** Fracture surfaces of A-286 tested at (a) 1180 °C; (b) 1200 °C; (c) 1220 °C.

With higher magnification, a film-like layer appears on the surfaces of grains, which is shown in Figure 3a, and their positions are associated with voids; however, these film-like phases and voids were not present in the as-heat treated microstructure, Figure 3b. It appears that film-like phases and voids were formed during the high temperature tensile test. The chemical composition of the film-like layer has been analyzed by SEM-EDAX and shown in Table 2. Although results indicate that the content of Ti is high, these film-like surfaces may be too thin to be isolated; therefore, major elements like iron, nickel and chromium, which belong to the substrate, have also been detected.

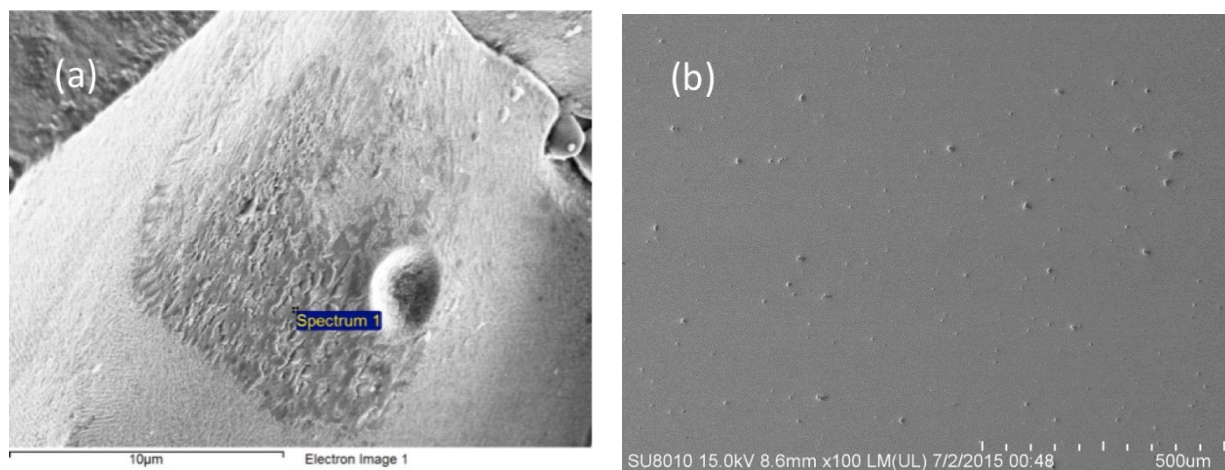


**Figure 3.** (a) Film-like precipitates on the inter-granular facets after 1220 °C tensile test; (b) as-heat treated microstructure.

**Table 2.** Chemical composition of Ti-rich precipitates via SEM-EDAX analysis in wt. %.

Element	Fe	Ni	Cr	Ti	Mn	Si	Al	O	C	P	S
wt. %	40.18	21.04	12.39	22.67	-	-	0.25	1.87	1.59	<0.01	<0.01

FIB was used to section TEM specimens from the film-like regions of the fracture surface shown in Figure 3a for TEM analysis. Figure 4a shows a cross-section containing both matrix and the surface layer. Their chemical compositions are shown in Table 3, and it is clear that the surface layer contains high level of Ti (A region, Figure 4b). On the other hand, the region beneath the top layer (B region) can be seen as A-286 matrix judging from the corresponding diffraction pattern, Figure 4c. Some elements were depleted, possibly due to the oxidation. The abrupt change in Ti content between the surface layer and the substrate indicates a phase boundary. Although the thickness of the Ti-rich layer is only about 100 nm, the area being enclosed can be around 50  $\mu\text{m}^2$  as shown in Figure 3a. The diffraction pattern taken for the Ti-rich phase is shown in Figure 4b and indicates a FCC structure with a lattice constant of 0.4398 nm, which is only slightly larger than the reported 0.4326 nm of TiC [14].

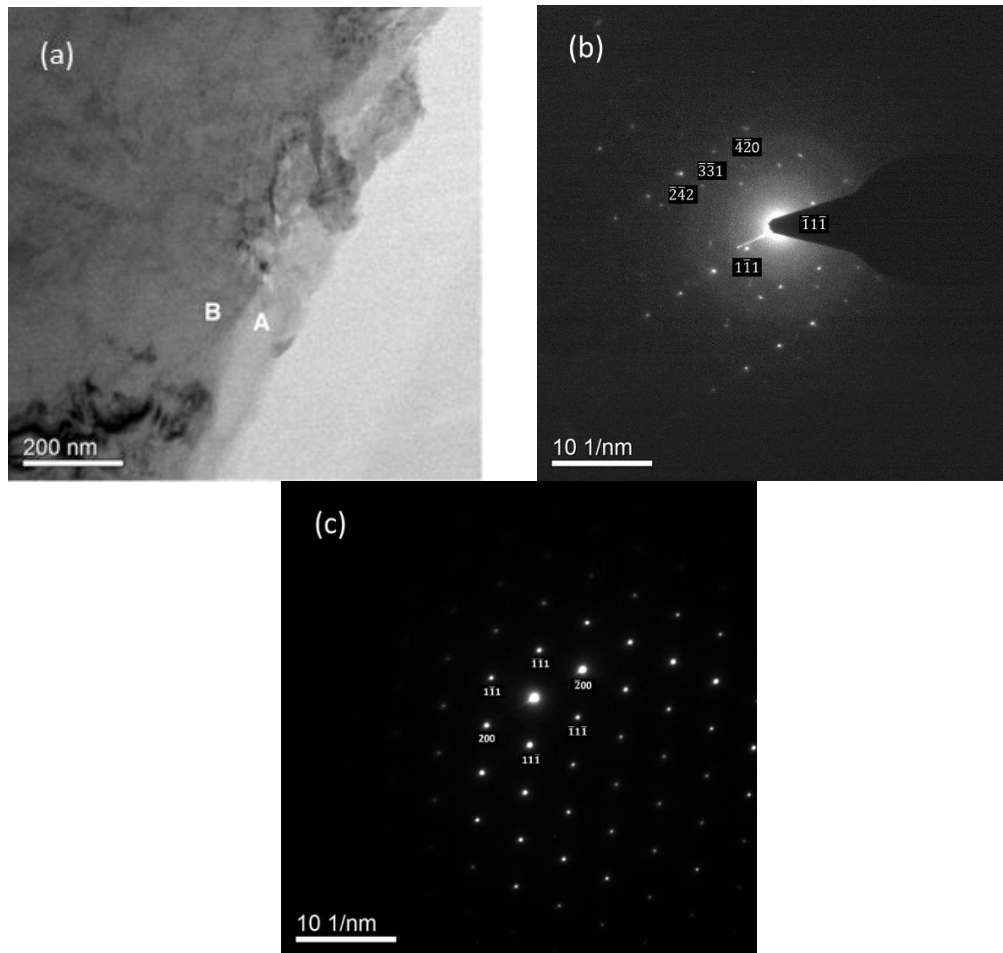


**Figure 4.** Transmission electron microscope analysis (TEM) analysis of A-286 tested at 1220 °C, (a) cross sectional view, and (b) diffraction pattern of the surface layer (A region), (c) diffraction pattern of the matrix (B region).

**Table 3.** TEM-EDS results in wt. %.

Site	Fe	Ni	Cr	Ti	Mn	Si	V	P	S
A	2.75	0.78	0.57	95.38	-	-	-	0.18	0.31
B	55.05	33.06	11.41	0.19	-	-	0.07	-	0.19

The interfaces between grain boundaries and phases within are known to be incoherent [15], and these interfaces are at higher energy state; therefore, impurities such as sulfur tend to segregate toward grain boundaries. Furthermore, TiC is often observed at the grain boundaries in A-286 [16]. Therefore, it is likely that TiC acts as a precursor for the formation of Ti-rich phase. Since the slightly higher level of sulfur and phosphorus are being detected in the Ti-rich phase, it is likely that both P and S react with TiC and form a lower melting temperature version of Ti-rich eutectic compounds. At 1220 °C, the Ti-rich eutectic compound may be liquefied and results in voids as shown in Figure 2c. Both voids and Ti-rich phase can lead to significant loss in ductility and inter-granular fracture. Upon subsequent cooling process, this Ti-rich phase would solidify as film-like appearance along the surfaces the grains, which were shown in Figures 3a and 4a.

To improve the high temperature ductility of A-286, one direct approach would be to further decrease the level of impurity so that formation of sulfur bearing Ti-rich phase can be hindered. Another approach is alloy design. With the addition of elements that can form stable sulfide, it may be able to prevent the formation of a low melting temperature phase; hence, the liquation phenomena can be prevented. Experimental work is ongoing to investigate the effect of elemental addition on sulfur segregation and the formation of Ti-rich phase.

#### 4. Conclusions

High temperature tensile tests have been conducted on Incoloy A-286 superalloy, and a ductile to brittle transition has been observed from 1180 to 1220 °C. Zero ductility has been observed at 1220 °C. Titanium-rich thin-film-like phase has been found on the inter-granular facets of the fracture surfaces. The present study indicates that, at 1220 °C, liquation of Ti-rich phase has caused thin-film-like morphology along the grain boundary and caused ductility loss during tensile deformation.

#### Acknowledgments

This research has been supported by the Industrial Technology Research Institute (ITRI), Taiwan. Authors appreciate Gloria Materials Cooperation for providing the ingot of Incoloy A-286.

#### Author Contributions

Chen-Wei Li, who conducts microstructure analysis and writes the first draft paper. An-Chou Yeh, who plans the research and assist in the writing of the manuscript. Chi-San Chen, who plans the research and prepare samples. Woei-Ren Wang, who plans the research and conduct tensile tests.

#### Conflicts of Interest

The authors declare no conflict of interest.

#### References

1. Kobayashi, K.; Yamaguchi, K.; Hayakawa, M.; Kimura, M. High-temperature fatigue properties of austenitic superalloys 718, A286 and 304L. *Int. J. Fatigue* **2008**, *30*, 1978–1984.
2. De Cicco, H.; Lупpo, M.I.; Raffaelli, H.; di Gaetano, J.; Gribaudo, L.M.; Ovejero-García, J. Creep behavior of an A286 type stainless steel. *Mater. Charact.* **2005**, *55*, 97–105.
3. De Cicco, H.; Lупpo, M.I.; Gribaudo, L.M.; Ovejero-García, J. Microstructural development and creep behavior in A286 superalloy. *Mater. Charact.* **2004**, *52*, 85–92.
4. Rho, B.S.; Hong, H.U.; Nam, S.W. Analysis of the intergranular cavitation of Nb-A286 alloy in high temperature low cycle fatigue using EBSD technique. *Scr. Mater.* **2000**, *43*, 167–173.
5. Chang, C.-M. Effect of Minor Elements on the Hot Deformation Behaviours of a Superalloy. Master Thesis, National Tsing-Hua University, Hsinchu, Taiwan, 2014.
6. Hansson, K.; Droujevski, M.; Fredriksson, H. Hot ductility of an Fe-10%Ni alloy during penetration of copper. *Scand. J. Metall.* **2002**, *31*, 256–267.

7. Heo, N.H. Sulfur segregation and intergranular fracture in  $\alpha$ -iron. *Scr. Mater.* **2004**, *51*, 339–342.
8. Mostefa, L.B.; Saindrenan, G.; Solignac, M.P.; Colin, J.P. Effect of interfacial sulfur segregation on the hot ductility drop of Fe-Ni36 alloys. *Acta Metall. et Mater.* **1991**, *39*, 3111–3118.
9. Osinkolu, G.A.; Kobylanski, A. The role of titanium additions on hot ductility of high purity iron base alloys. *Scr. Metall.* **1987**, *21*, 243–247.
10. Yu, Y.; Chen, W.; Zheng, H. Research on the hot ductility of Fe-36Ni invar alloy. *Rare Met. Mater. Eng.* **2014**, *43*, 2969–2973.
11. Abbasi, S.M.; Morakabati, M.; Mahdavi, R.; Momeni, A. Effect of microalloying additions on the hot ductility of cast FeNi36. *J. Alloys Compd.* **2015**, *639*, 602–610.
12. Santillana, B.; Boom, R.; Eskin, D.; Mizukami, H.; Hanao, M.; Kawamoto, M. High-temperature mechanical behavior and fracture analysis of a low-carbon steel related to cracking. *Metall. Mater. Trans. A* **2012**, *43*, 5048–5057.
13. Ducki, K.J.; Hetmańczyk, M.; Kuc, D. Analysis of the precipitation process of the intermetallic phases in a high-temperature Fe-Ni austenitic alloy. *Mater. Chem. Phys.* **2003**, *81*, 490–492.
14. El-Eskandarany, M.S. Structure and properties of nanocrystalline TiC full-density bulk alloy consolidated from mechanically reacted powders. *J. Alloys Compd.* **2000**, *305*, 225–238.
15. Yoo, K.-B.; Kim, J.-H. Effects of impurity segregation to grain boundary on intergranular cracking in 2.25Cr-1W steel. *Procedia Eng.* **2011**, *10*, 2484–2489.
16. Zhao, M.J.; Guo, Z.F.; Liang, H.; Rong, L.J. Effect of boron on the microstructure, mechanical properties and hydrogen performance in a modified A286. *Mater. Sci. Eng. A* **2010**, *527*, 5844–5851.

© 2015 by the authors; licensee MDPI, Basel, Switzerland. This article is an open access article distributed under the terms and conditions of the Creative Commons Attribution license (<http://creativecommons.org/licenses/by/4.0/>).